PERGAMON

Journal of Structural Geology 23 (2001) 379–392

JOURNAL OF STRUCTURAL GEOLOGY

www.elsevier.nl/locate/jstrugeo

Transverse fold evolution in the External Sierra, southern Pyrenees, Spain

David J. Anastasio*, James E. Holl[1]

Department of Earth and Environmental Sciences, Lehigh University, Bethlehem, PA 18015-3188, USA

Received 25 January 2000; accepted 29 June 2000

Abstract

Fault-slip data are used to reconstruct varying tectonic regimes associated with transverse fold development along the eastern and southern margins of the Jaca basin, southern Pyrenees, Spain. The Spanish Pyrenean foreland consists of thrust sheets and leading-edge décollement folds which developed within piggyback basins. Guara Formation limestones on the margins of the Jaca basin were deposited synchronously with deformation and are exposed in the External Sierra. Within the transverse folds, principal shortening axes determined from *P* and *T* dihedra plots of fault-slip data show a shift from steep shortening in stratigraphically older beds to NNE–SSW horizontal shortening in younger beds. Older strata are characterized by extensional faults interpreted to result from halotectonic (salt tectonics) deformation, whereas younger strata are characterized by contraction and strike-slip faults interpreted to result from thrust sheet emplacement. The interpretation of the timing for the shortening axes in the younger strata is supported by the observation that these axes are parallel to shortening axes determined from finite strain analysis, calcite twins, and regional thrusting directions determined from fault-related folds and slickenlines. This study shows that fault population analysis in syntectonic strata provides an opportunity to constrain kinematic evolution during orogeny.

1. Introduction

The External Sierra along the southern margin of the Jaca piggyback basin, southern Pyrenees, Spain, are characterized by large-scale transverse folds (Fig. 1). The folds were attributed to emplacement of more easterly thrust sheets (Séguret, 1972; Garrido-Megias and Camara, 1983), to fault-related folding above a westward imbricating oblique ramp (Déramond and Hossack, 1984; Nichols, 1984; Hirst and Nichols, 1986), and to differential loading halotectonics (salt tectonics) in response to westward sediment progradation in the piggyback basin (Anastasio, 1992). Synorogenic flysch and mollase deposited within the Jaca basin were used to establish the timing of sedimentation and deformation (Hogan and Burbank, 1996; Pueyo et al., 2000). In this paper, fault-slip data from synorogenic carbonate rocks deposited along the Jaca basin margins (Guara Formation) are used to reconstruct the tectonic regimes associated with the transverse fold development.

Kinematic assessments from strain analysis and asymmetric microstructures can provide important information on fault displacements and folding mechanisms (e.g. Boyer, 1978; Anastasio et al., 1997); however, penetrative tectonites are generally absent from external thrust zones. Foreland deformation commonly results in penetrative fault and joint systems, which have been used as a record of deformation kinematics (e.g. Appalachians: Nickelsen and Hough, 1967; Wojtal, 1986; Canadian Rockies: Price, 1967; US Rockies: Stearns, 1969; Pyrenees: Hancock, 1985; Turner and Hancock, 1990; Taiwan: Angelier et al., 1986; Himalayas: Thomas et al., 1996). In syntectonic deposits, fault populations have the potential to record temporal variations in deformation kinematics during orogenesis (e.g. Kleinspehn et al., 1989).

Empirical studies of fault-slip data have been used to infer deformation geometry, finite rotations, fault displacements, and plate convergence directions (e.g. Angelier et al., 1986; Gapais et al., 2000; Rocher et al., 2000). Kinematic interpretations of fault-slip data have been facilitated by both numerical (e.g. Etchcopar et al., 1981; Angelier, 1990) and graphical (e.g. Angelier and Mechler, 1977; Marrett and Allmendinger, 1990) approaches. Inversion methods utilize numerical computations to search for the best fit between fault-slip data and an unknown deformation tensor, but for heterogeneous fault populations, a unique solution may be elusive (Angelier, 1994). The graphical *P* and *T* dihedra method (Angelier and Mechler, 1977), on the other hand, assumes that the principal axes lie somewhere

* Corresponding author. Tel.: 001-610-758-5117; fax: 001-610-758-3677.

E-mail address: dja2@lehigh.edu (D.J. Anastasio).

[1] Present address: ExxonMobil Upstream Research Company, Houston, TX 77252-2189, USA.

0191-8141/01/$ - see front matter
PII: S0191-8141(00)00102-4

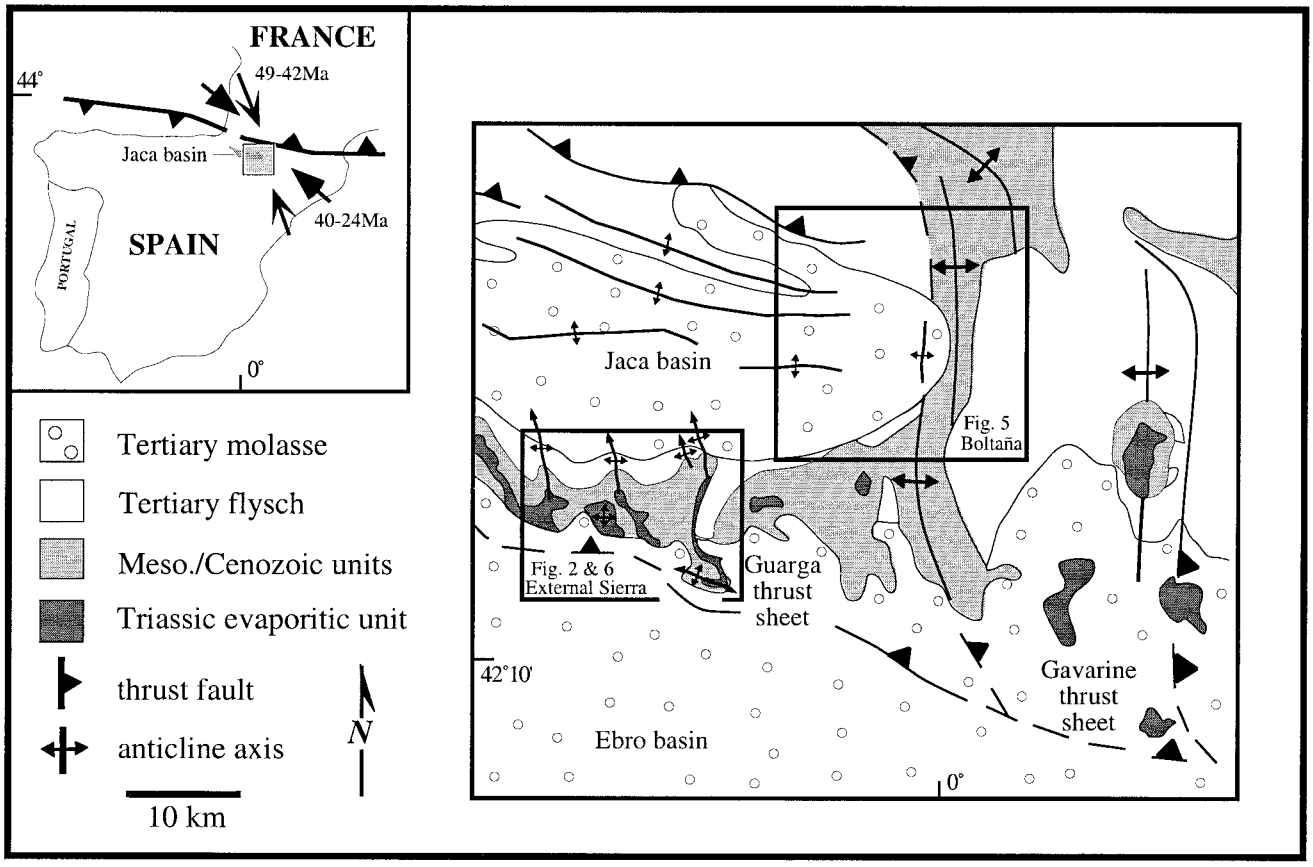

Fig. 1. Map of the eastern Jaca basin showing the location of the Boltaña (Fig. 5) and External Sierra field sites (Fig. 6). Inset shows convergence direction between Iberia and Eurasia for 49–42 Ma and 40–24 Ma (Roest and Srivastava, 1991).

in the *P* and *T* quadrants of a pseudo-focal mechanism solution for a single fault datum (MacKenzie, 1969). Kinematic axes for a fault population are arrived at by combining faults of different orientations whose principal axes partially overlap those of the other faults. The orientations that have the maximum overlap of *P* and *T* quadrants are assumed to contain the greatest and least principal strain axes, respectively (Marrett and Allmendinger, 1990). We chose the more robust and simplier *P* and *T* dihedra method to derive strain axis orientations for fault populations, which we then used to evaluate the evolution of transverse folding in the Spanish Pyrenean foreland.

2. The Spanish Pyrenees

The Pyrenees formed as a consequence of the Cretaceous–Miocene collision of the Iberian microplate with the Eurasian plate (Choukroune and Séguret, 1973; Roest and Srivastava, 1991). Orogenic shortening east of 1° 20′ west longitude was accommodated by limited subduction of lower Iberian crust beneath Eurasian crust (ECORS Pyrenees Team, 1988), whereas to the west of 1° 40′ west longitude, Eurasian crust of the Bay of Biscay was subducted beneath the Iberian margin (e.g. Daignieres et al., 1981; Grimaud et al., 1982). The Pyrenees are a doubly vergent thrust belt, which shortened the plate margins by ~50% (~147 km in the central sector), with the majority of the shortening directed southward (Roure et al., 1989; Muñoz, 1992). The Spanish Pyrenees consists of a two-tiered thrust network. A lower basement duplex with a roof thrust in Triassic evaporites served as the décollement for the upper-tier thrust sheets, which carried the preorogenic roof sequence and synorogenic piggyback basins southward (Cámara and Klimowitz, 1985; Déramond et al., 1985).

During Alpine compression, tectonic inversion of Mesozoic basins produced a wide low-tapered foreland composed of several large thrust sheets (Séguret, 1972). The west central foreland includes the Gavarine and Guarga thrust sheets of the South Pyrenean zone and the External Sierra zone (Cámara and Klimowitz, 1985; Teixell, 1996). These thrust sheets contain leading imbricate fans and extensive décollement folds along their southern margins (Almela and Rios, 1952; DePaor and Anastasio, 1987; Anastasio, 1992; Meigs, 1997). The regional thrusts are listric in shape with steep footwall cut-offs near the synorogenic surface (~50°). The imbricate thrusts of the Guarga thrust sheet became emergent on the synorogenic surface during emplacement.

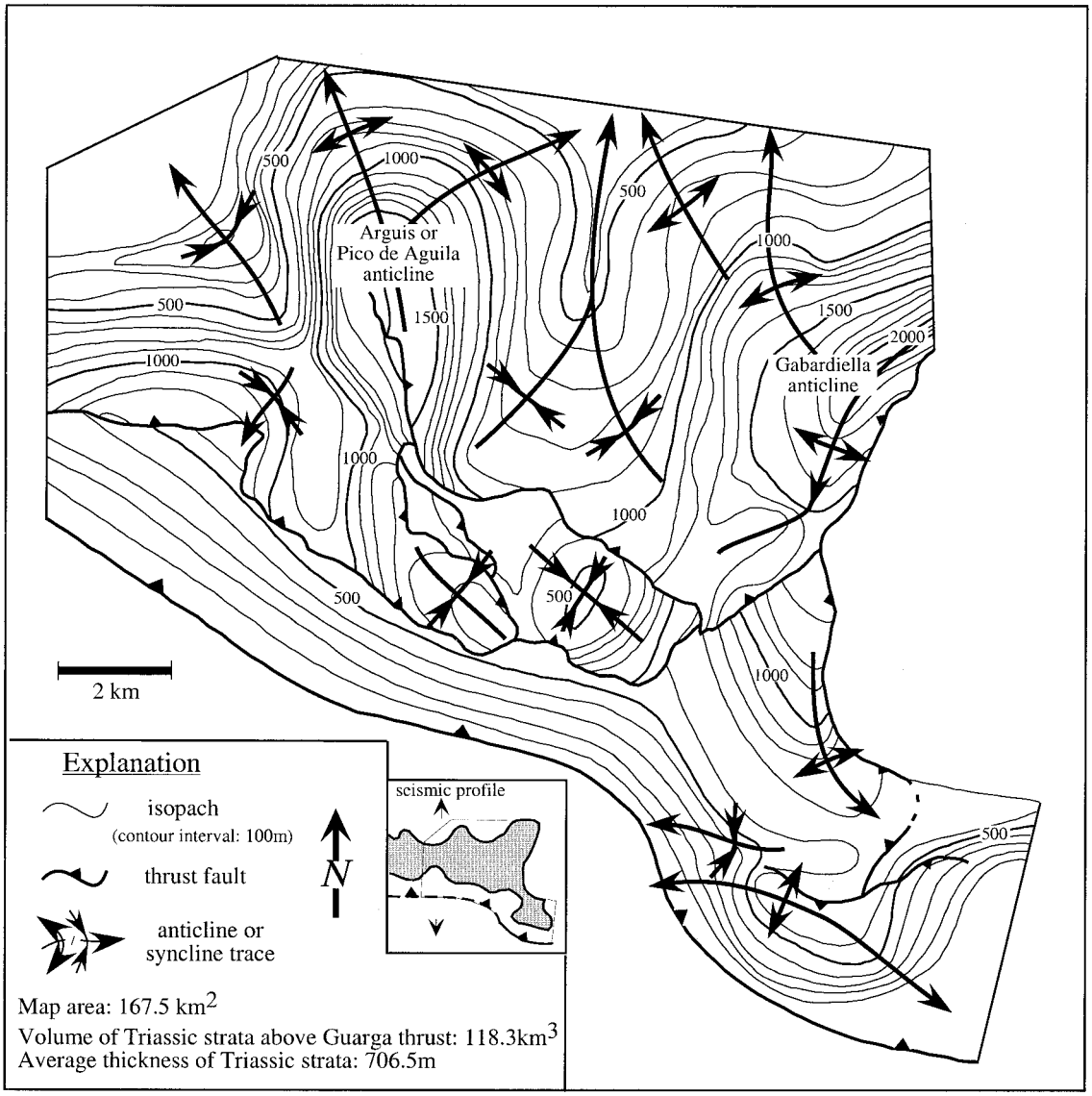

Fig. 2. (a) Triassic stratigraphic thickness in the hanging wall of the Guarga thrust (location shown in Fig. 1). The bottom of the volume is the Guarga thrust projected along strike from its migrated position on reflection seismic records [collected by Prakla Seismos (Germany) along old route N-136 from Huesca to Jaca over Monrepos pass in 1977, processed by PGG (France), and provided by REPSOL (Spain)]. The volume top is the Triassic–Cretaceous unconformity constructed from geologic map information and measured sections (Anastasio, 1987).

Stratigraphic relationships within synorogenic deposits document the hindward progression of the Guarga-leading imbricate fan (Anastasio, 1992).

The décollement zone of the Guarga thrust sheet is variable in thickness, depending on whether the mobile evaporite-rich Keuper facies evacuated to produce salt welds or collected beneath concordant décollement anticlines (Fig. 2). In places, the décollement zone comprises a thick (many hundreds of meters) broken formation with large isolated carbonate (Mushelkalk Facies) blocks (Mey et al., 1968; Zwart, 1979), diabase pieces, or cavernous and brecciated dolomites (Fig. 3). This dolomite texture is thought to represent the tectonic deformation of evaporite-bearing carbonate rocks (Müller, 1982; Diegel, 1988).

Atop the Guarga thrust sheet, the Jaca piggyback basin accumulated thick flysch and molasse deposits, while basin margins and active areas of internal uplift accumulated shallow marine carbonate (Guara Formation) (Puigdefabregas, 1975; Labaume et al., 1985; Barnolas and Teixell, 1994). The synorogenic sediments of the Jaca basin were faulted and deformed into east-trending folds and faults. To the south, however, within the External Sierra and east, near Boltaña, transverse (transport-parallel, north-trending) folds dominate (Fig. 1). Boltaña anticline is a regional-scale, west-vergent, asymmetric anticline located above the western oblique ramp of the Gavarine thrust sheet (Holl and Anastasio, 1995a). The folds of the External Sierra consist of broad flat-bottomed synclines and tight symmetric anticlines developed along the frontal imbricate of the Guarga thrust sheet. The folds become smaller in

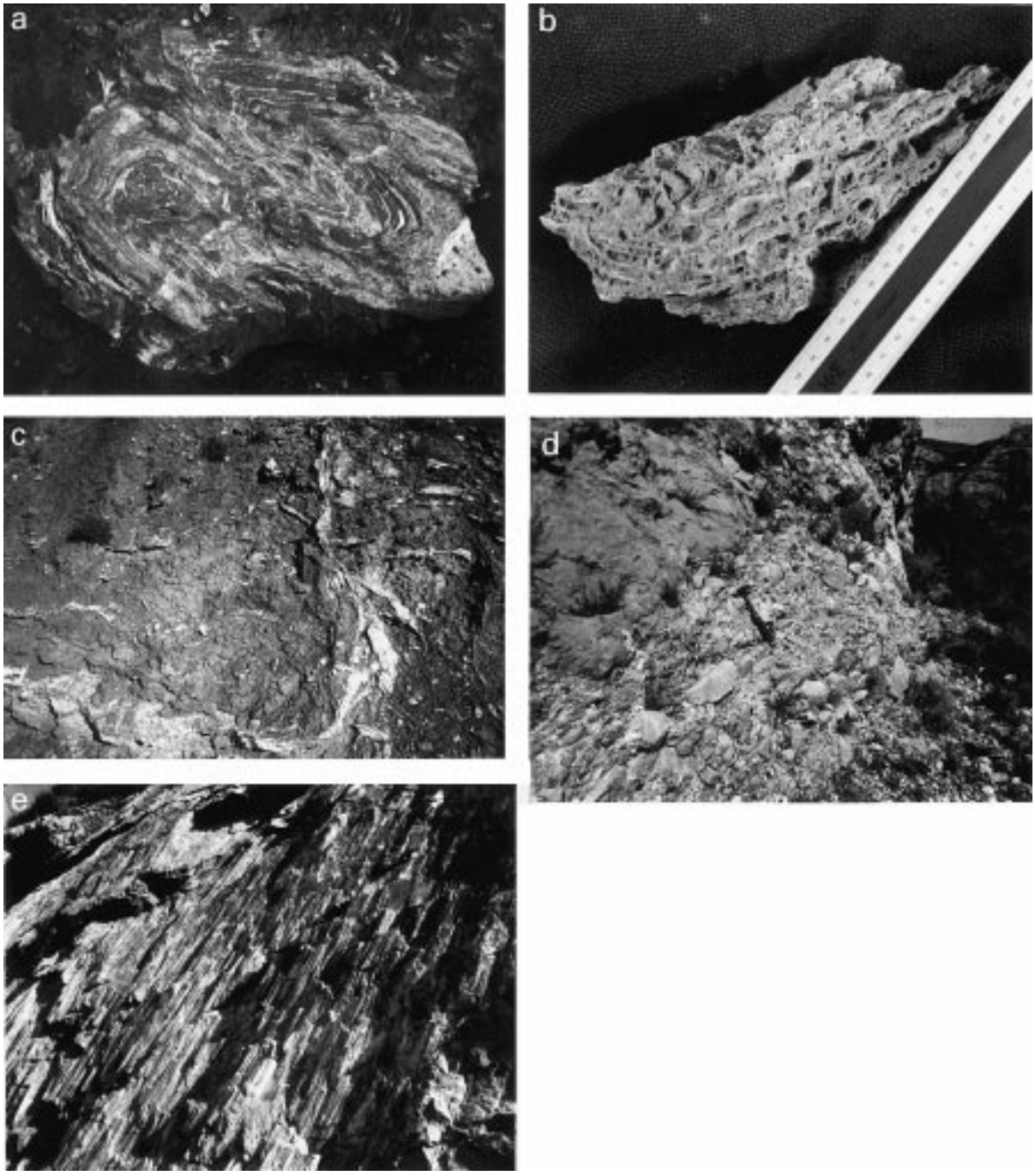

Fig. 3. (a) Block of brecciated and folded Mushalkalk limestone (50 cm wide) in shale matrix, with white gypsum veins visible. (b) Hand sample of cellular dolomite abundant in Mushalkalk facies in External Sierra; scale in cm. (c) Outcrop photo of typical Keuper gypsiferous shale near the base of the Guarga thrust (hammer for scale). (d) View east along thrust front towards Salto de Roldan; footwall ramp in horizontal molasse visible in background. Foreground exposes emergent imbricate of the Guarga thrust. Brecciated Cretaceous hanging wall center foreground above undeformed Miocene clastics right (hammer for scale). (e) Typical calcite shear fibers on a backthrust surface at station 11 (hammer parallel to fibers for scale).

amplitude and generally younger westward (Puigdefabregas, 1975). The transverse External Sierra and Boltaña folds developed synchronous with westward synorogenic sedimentation within the foreland basin (Anastasio, 1992). A halotectonic origin for the transverse folds is supported by the irregular fold geometries (Fig. 2), the ubiquitous evaporitic strata along the décollement (Contribucion de la Exploracion Petrolifera al Conocimiento de la Geologia de Espana, 1987), and in the fold cores (Fig. 3), the timing of folding (Fig. 4), and palinspastic restorations of the folds and Jaca basin sedimentation (Anastasio, 1992).

The eastern, earlier formed folds of the Jaca basin localized thrust trajectories, whereas western folds within the piggyback basin grew contemporaneously with Guarga thrust

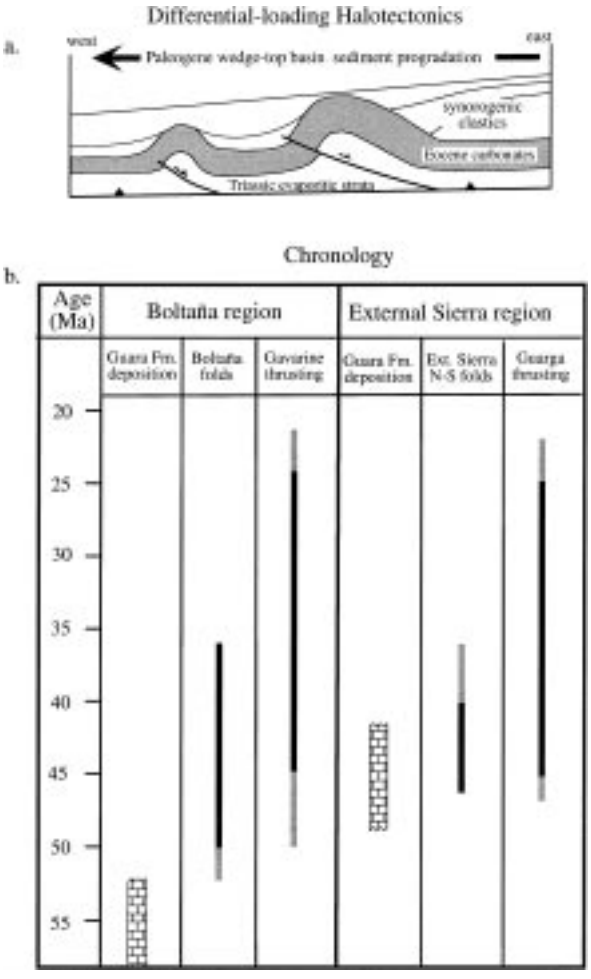

Fig. 4. (a) Schematic development of transverse décollement folds produced by differential-loading halotectonics in the Jaca basin (after Anastasio, 1992). (b) Deposition and deformation chronologies for the southeastern Jaca basin; gray bars for age uncertainties.

sheet emplacement (Anastasio, 1992) (Fig. 4). The transverse folds ceased amplification in the early Oligocene, while thrusting persisted along the thrust front until the early Miocene (Anastasio, 1992; Hogan and Burbank, 1996; Meigs, 1997). Emplacement of the Guarga thrust sheet occurred from 46 to 22–24.5 Ma, with displacement diminishing westward from 12 km near Arguis (Pico del Aguila) anticline (DePaor and Anastasio, 1987) to 8 km near Rio Gallego, 28 km to the west (Puigdefabregas, 1975).

3. Methodology

To refine the deformation history of Pyrenean foreland interpreted from synsedimentary structural geometries, we investigated mesoscopic faults (>600 faults) in Eocene Guara Formation carbonates from several large-scale transverse folds exposed along the southern margin (Arguis or Pico de Aguilla and Gabardiella anticlines) and eastern margin (Boltaña anticline) of the Jaca basin (Figs. 5 and 6). Stations were selected to sample various structural and stratigraphic positions within the transverse folds. At each of 11 stations, all located along road-cuts which provide good three-dimensional exposure, all faults with exposed lengths >10 cm were measured and subsequently analyzed (Figs. 5 and 6). The direction and sense of fault displacement was determined from fault surface features, typically stepped shear fibers (e.g. Durney and Ramsay, 1973) (Fig. 2e). Because the faults are in massive carbonates, fault displacements or surface areas were untenable, so all faults were assumed to be of equal displacement magnitude in subsequent analysis. Few data are available on the relative age of fault motions within each outcrop, as cross-cutting faults are rare and very few faults (~1%) record multiple or varying slip directions. However, the kinematic evolution of the transverse folds can be reconstructed by comparing fault populations from different stratigraphic positions within the syntectonic Guara Formation.

Measured fault populations were used to constrain station kinematics in several ways. Block-diagram perspectives of fault populations were constructed to illustrate the orientation and displacement patterns of the faults (Figs. 7 and 8). The block diagrams provide a clear display of fault kinematic variations and relative abundance of various fault types as a function of structural and stratigraphic position. The block diagrams used results from slip-linear plots, which are stereographic projections of fault poles and their surrounding trace of the plane defined by a fault pole and a slip direction (M-plane) labeled to indicate the direction of hanging wall motion (Hoeppener, 1955).

Graphical analysis using the P and T dihedra method constrained the orientation of the principal strain axes most consistent with the fault populations at each station (Figs. 9 and 10) (program FaultKin, Allmendinger et al., 1992). Strain axis orientations were improved by including large numbers of faults of diverse orientations (e.g. Lisle, 1987; Angelier, 1994), by sampling multiple structural and stratigraphic positions, and by isolating nonsystematic faults (program PSALMS, Will and Powell, 1991). At all sampling stations, the ratio between the number of kinematically compatible faults and the total number of faults averages 80% (±5% standard deviation; Figs. 5 and 7).

4. Results

4.1. Fault populations in Boltaña anticline

In Boltaña anticline, a diversity of fault types exists at each station, with normal faults and strike-slip faults dominating in abundance (Figs. 5 and 7). On the backlimb of Boltaña anticline (stations 3, 4, and 7), normal faults are generally north or northeast striking and dip to the south or southeast. Strike-slip faults are both sub-parallel and sub-perpendicular to the anticlinal axis, dip steeply, and are both left- and right-lateral. Hinge regions of Boltaña

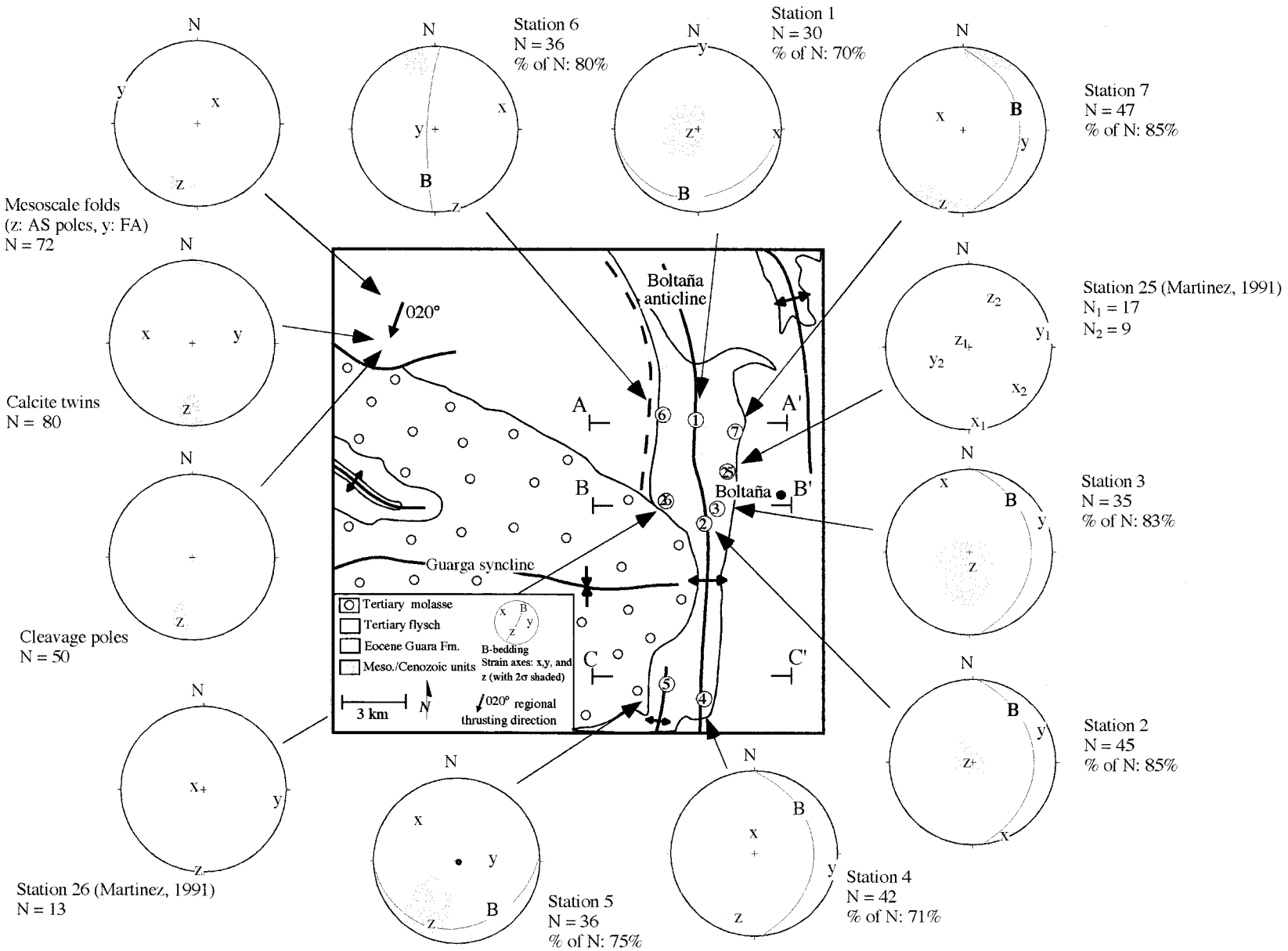

Fig. 5. Simplified geologic map of Boltaña region (see Fig. 1 for location) showing fault stations and principal strain axes derived from fault population analysis. Stations numbered from stratigraphic oldest to youngest except stations 25 and 26 from Martinez (1991). Fold, calcite twin, and cleavage data from Holl and Anastasio (1995b). Number of measured faults and percentage of displacements consistent with strain axes are indicated. Gray pattern: 2σ standard deviation of Kamb contour. Locations of Fig. 9 cross-sections A, B, and C are shown.

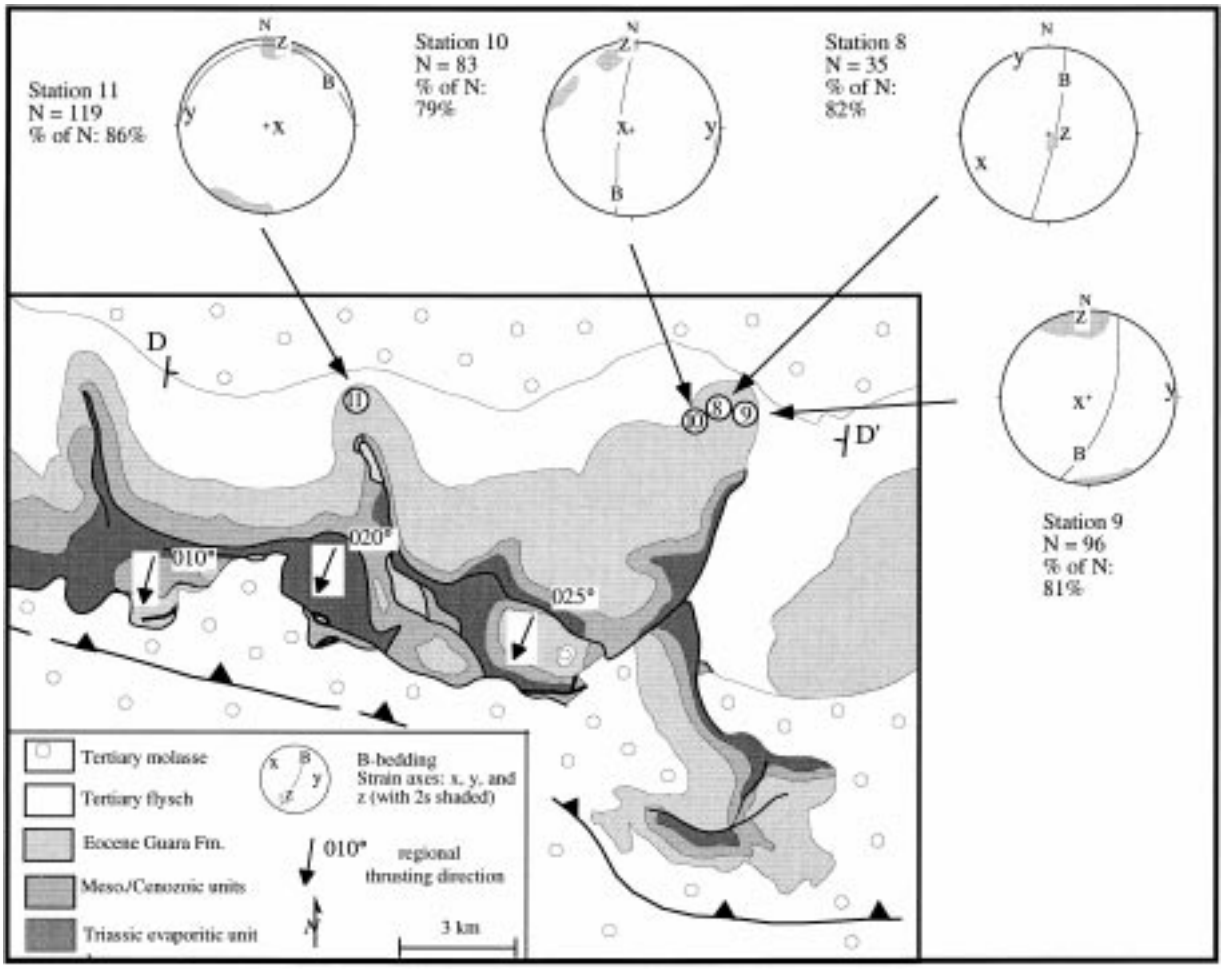

Fig. 6. Simplified geologic map of a portion of the External Sierra (see Fig. 1 for location) showing fault stations and principal strain axes derived from fault population analysis. Stations numbered from stratigraphic oldest to youngest. Number of measured faults and percentage of displacements consistent with strain axes are indicated. Gray pattern: 2σ standard deviation of Kamb contour. Location of Fig. 10 cross-section D is shown.

anticline (stations 1, 2, and 5) contain either strike-parallel (stations 1 and 5) or strike-perpendicular extensional faults (station 2). Right-lateral strike-slip faults occur in greater abundance than left-lateral strike-slip faults at stations 2 and 5 where normal-oblique, and contractional faults also occur. Extensional and strike-slip faults in the forelimb of the Boltaña anticline (station 6) are dominantly northeast striking and dip both to the southeast and northwest. In stratigraphically older stations (e.g. stations 1 and 3), normal faults with variable orientations predominate, whereas up-section, there is a larger contribution from contractional faults (e.g. stations 6 and 7; Fig. 7).

In Boltaña anticline, P axes (= shortest axis of finite strain, z) are near vertical for stratigraphically older positions (e.g. stations 1, 2, and 3) irrespective of position on the fold and nearly horizontal at 004–184° for stratigraphically younger positions (e.g. stations 4, 5, 6, and 7; Figs. 5 and 9). In strata younger than the Eocene Guara Formation, principal shortening axes of bulk finite strain determined from Fry analysis of framework grains (005°–030°), twin analysis (010°–025°), and normals to mesoscopic fold axes (010°–030°) are all sub-parallel with thrust translation directions (020° towards 200°) inferred from fault-related folds and slickenlines (Fig. 5). The exception is in the vicinity of the western oblique ramp of the Gavarnie thrust sheet, where shortening axes are normal to the ramp for 20 km in the hanging wall and 10 km in the footwall (see Holl and Anastasio, 1995a).

4.2. Fault populations in the External Sierra

In the External Sierra, stations 8, 9, and 10 are located on the limbs of Gabardiella anticline, and station 11 is located on the hinge of Arguis (Pico del Aguila) anticline (Figs. 2 and 10). Again, the External Sierra stations display a diversity of fault types (Figs. 6 and 8), but faulting varies little with respect to structural position about the tight transverse folds (stations 9, 10, and 11). In the lowest stratigraphic position (station 8), strike-parallel extensional faults with apparent thrust offset of steep bedding and strike-slip faults

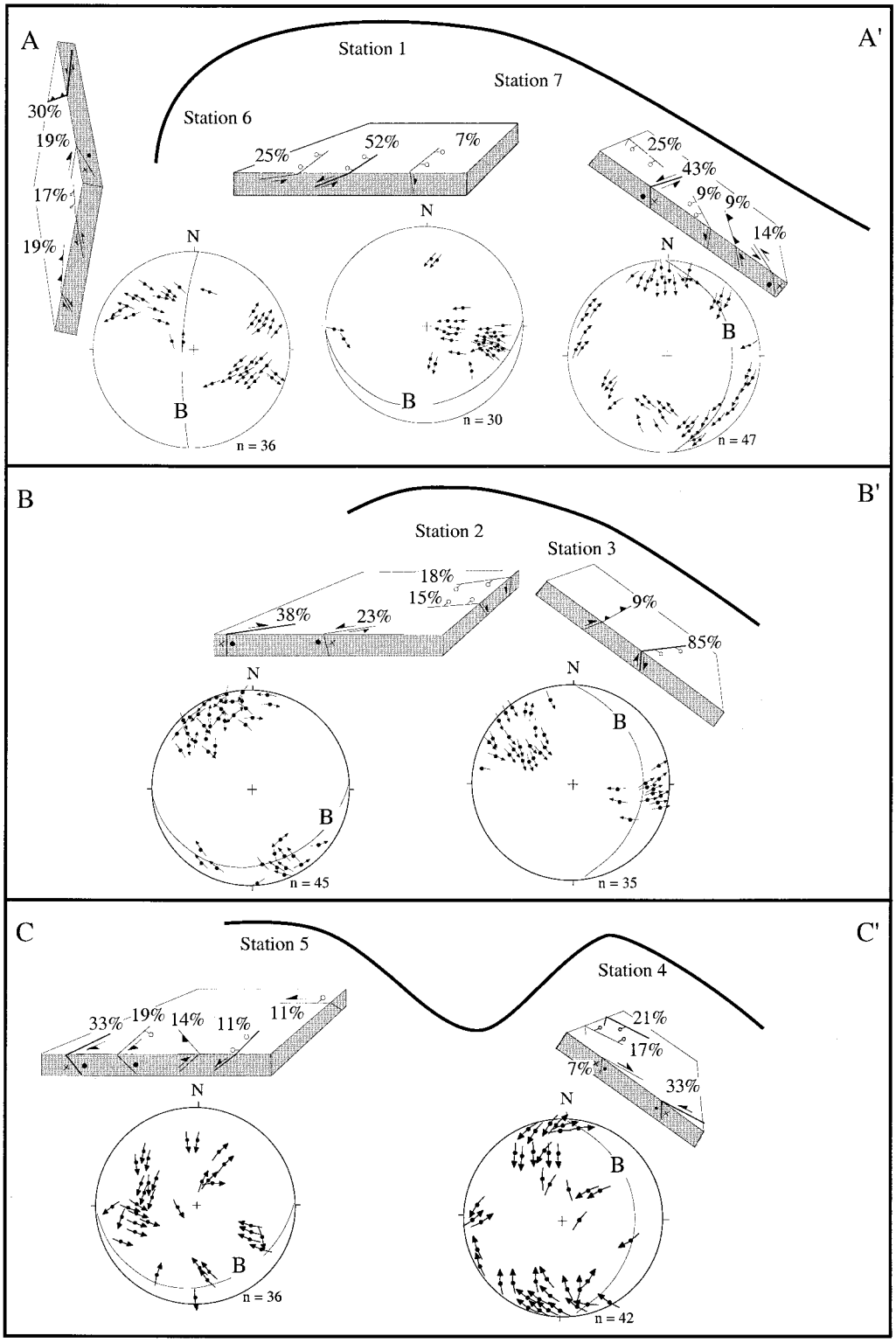

Fig. 7. Bedding form lines for cross-sections AA′, BB′, and CC′ through Boltaña anticline (locations in Fig. 5). For each station, a block diagram oriented as bedding shows relative abundance of mesoscopic fault types in percentages with lower hemisphere stereographic projections of fault slip linears. B: bedding. Faults with solid barbs: contraction faults (sensu Norris, 1958); faults with open circles: extension faults (sensu Norris, 1958); faults with dot and x-strike-slip faults: dot outward motion, × inward motion.

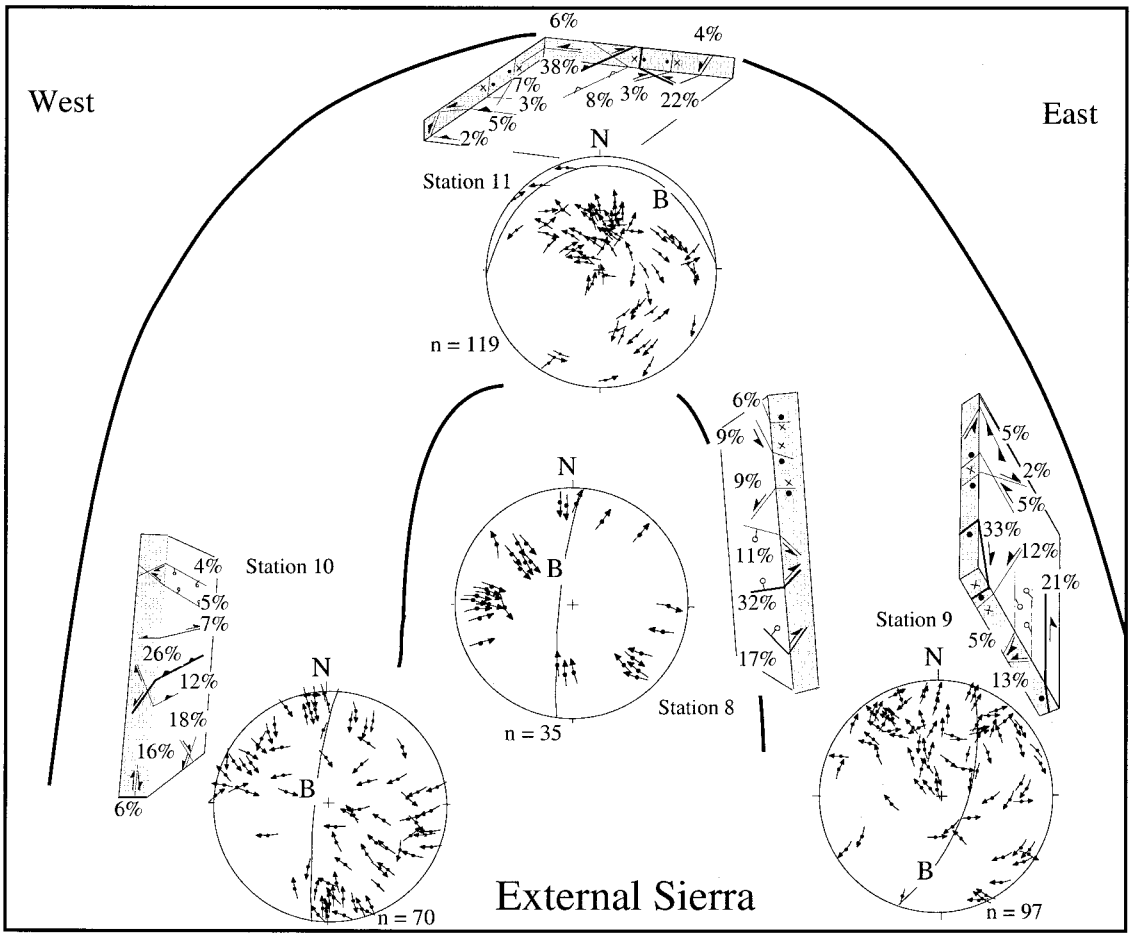

Fig. 8. Bedding form lines for composite reconstruction of an External Sierra, transverse halotectonic décollement fold using stations 8–11 along cross-section DD′ (location in Fig. 6). For each station, a block diagram oriented as bedding shows relative abundance of mesoscopic fault types in percentages with lower hemisphere stereographic projections of fault slip linears. B: bedding. Faults with solid barbs: contraction faults (*sensu* Norris, 1958); faults with open circles: extension faults (*sensu* Norris, 1958); faults with dot and x-strike-slip faults: dot outward motion, × inward motion.

dominate in abundance. At other limb stations (9 and 10), strike-parallel contraction faults with normal offsets in geographic coordinates and strike-slip faults dominate, with the proportion of contraction faults increasing up-section (Fig. 8). Conjugate strike-parallel normal faults also occur at limb stations 9 and 10. Many contraction faults are backthrusts that shorten bed lengths perpendicular to the fold axis and a majority of the strike-slip faults are fold axis parallel (Fig. 8).

The *P*–*T* dihedra plots (Fig. 10) show a steep shortening axis at station 8, the stratigraphically oldest of the External Sierra and nearly horizontal shortening axes trending 002–182° at the higher stratigraphic levels exposed at stations 9, 10, and 11. At stations 9, 10, and 11, horizontal shortening axes (*z* axes in Fig. 6, *P* axes in Fig. 10) are associated with vertical extensions (*x* axes in Fig. 6, *T* axes in Fig. 10), whereas, at station 8, a vertical shortening axis is associated with extension plunging shallowly towards 240° (Figs. 6 and 10).

Given the great diversity of fault types and the large region studied, the kinematic analysis of the fault slip produced remarkably consistent strain axis orientations (Fig. 11). Stratigraphically older strata within both the Boltaña and External Sierra regions are characterized by steep shortening, whereas younger strata are characterized by horizontal, NNE–SSW-oriented shortening, regardless of structural position.

5. Interpretation

In regions undergoing brittle deformation, a diversity of coeval fault types commonly exist (e.g. Hancock, 1985; Aydin and Reches, 1982; Holl and Anastasio, 1992). When interpreting fault populations in the southern Pyrenees, we sought explanations consistent with the structural styles typical of foreland thrust belts and of halotectonic deformations: In thrust belts, contractional faults (sensu Norris, 1958) typically verge towards the foreland, but backthrusts also occur (e.g. Dahlstrom, 1970). Mesoscopic contractional faults can accommodate distributed layer-parallel shortening (e.g. Cloos, 1961). In thrust belts with

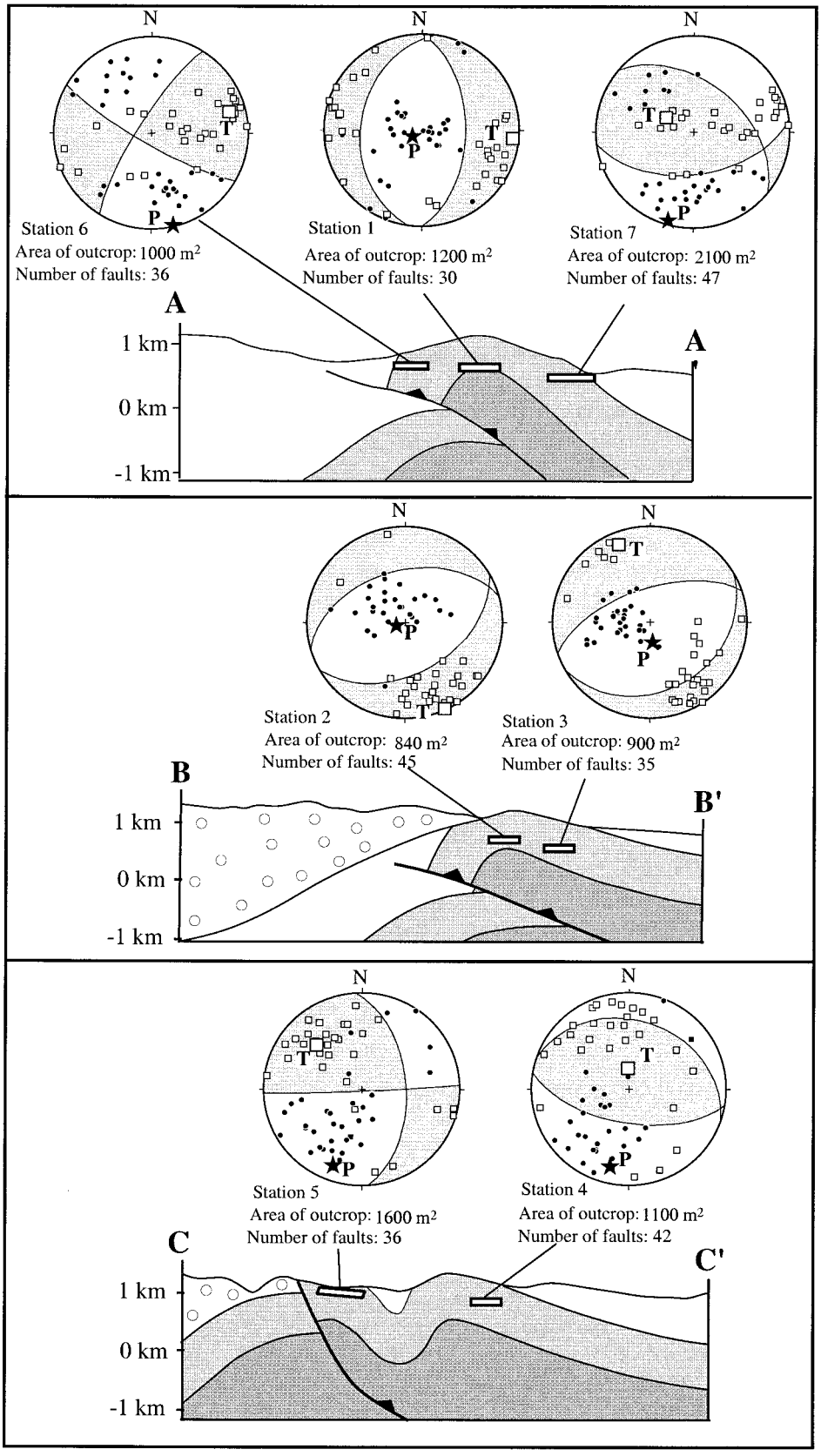

Fig. 9. Simplified cross-sections AA′, BB′, and CC′ of the Boltaña region (locations in Fig. 5). Rectangles show fault measurement sites; outcrop area and number of faults analyzed are also indicated. Lower-hemispheric stereographic projections show results of *P*–*T* dihedra plots of fault kinematic data. Compression (*P*) and tension (*T*) axes inferred from each fault and most likely principal compression axis (star) and principal tension axis (square) are shown for each station.

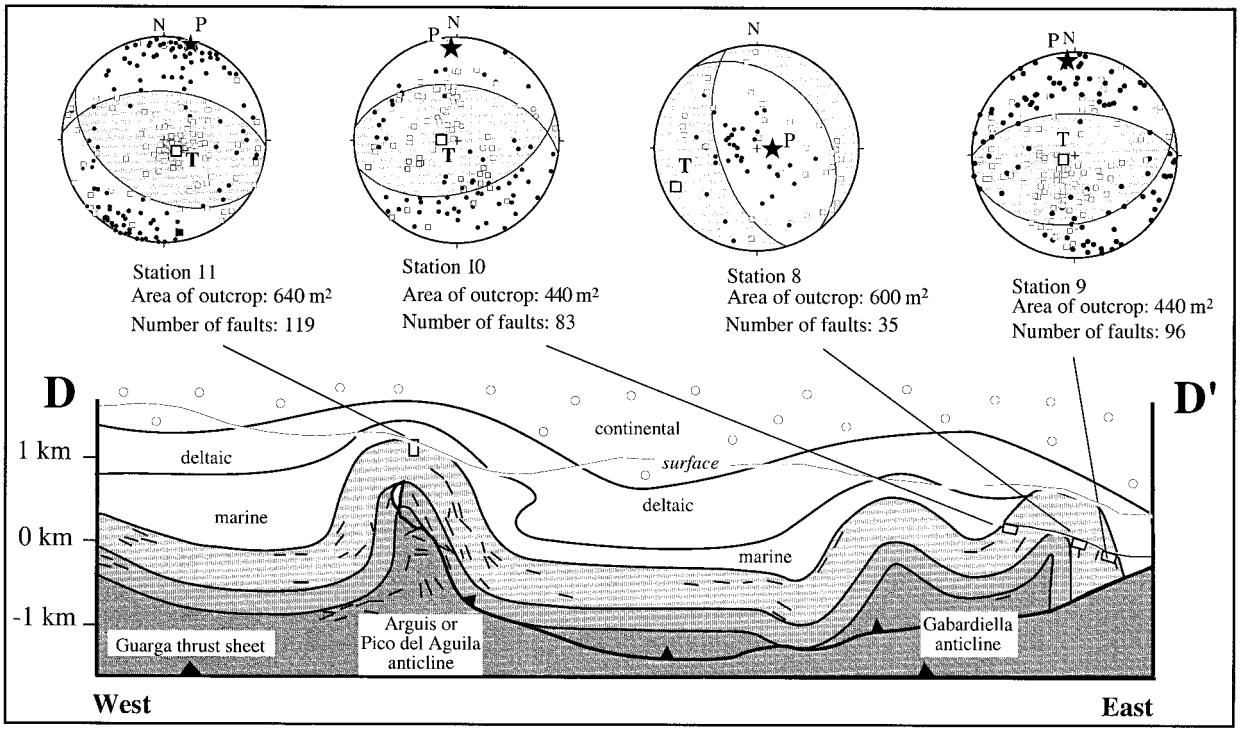

Fig. 10. Strike-parallel cross-section through the External Sierra region; short bold lines represent bedding traces down-plunge projected onto a vertical plane trending100–280°, current surface along section line (located in Fig. 6) indicated. Rectangles show fault measurement sites; outcrop area and number of faults analyzed are also indicated. Lower-hemispheric stereographic projections show results of *P–T* dihedra plots of fault kinematic data. Compression (*P*) and tension (*T*) axes inferred from each fault and most likely principal compression axis (star) and principal tension axis (square) are shown for each station.

thick evaporite-rich décollements, folding is more common than thrusting, and both folds and thrusts lack consistent foreland vergence (Davis and Engelder, 1987; Jackson and Talbot, 1994). Strike-slip faulting in thrust belts is common and has been related to lateral displacement gradients (e.g. tear faults, Dahlstrom, 1970) and to strain patterns (converging and diverging flow) within thrust sheets (e.g. Price, 1967; Bielenstein, 1969). Extensional faults (*sensu* Norris, 1958) in thrust belts generally postdate some contraction, verge towards the foreland, and accommodate thinning of a thrust sheet (e.g. Wojtal, 1986) or of the entire thrust wedge (Dahlen et al., 1984). Salt domes occur in both extensional and compressional tectonic provinces (e.g. Jackson and Talbot, 1994), where halotectonic folds are characterized by extensional faults of varying orientations (e.g. Schwerdtner et al., 1978; Jenyon, 1986).

Along the southern and eastern margins of the Jaca basin, we found a diversity of fault types at each station but few consistent displacement patterns with structural position (Figs. 7 and 8). Given the complexity of Pyrenean deformation, including varying Tertiary Iberian–Eurasian convergence directions (Fig. 1), complex foreland folding (Fig. 2), local variations in strain (e.g. Holl and Anastasio, 1995b), and local thrust sheet rotations (e.g. Hogan and Burbank, 1996), this result is not surprising. Contraction faults dominate in abundance at a hinge station 11, where backthrusts are most common, and at limb stations 6 and 10, where west-vergent faults dominate, but few faults mimic regional thrusting directions, which vary from 190° to 205° in the areas studied (Figs. 5 and 6). Strike-slip faults occur at most stations, but orientation and displacement sense vary widely with respect to both structural and stratigraphic position.

The complex fault patterns (Figs. 7 and 8) and the tendency for multiple fault sets to develop simultaneously (Reches, 1978; Aydin and Reches, 1982; Wojtal, 1986; Krantz, 1988) led us to a strategy of considering the overall distortion accommodated by faulting at each station. Internal consistency of the principal strain axes determined by the *P* and *T* dihedra plots (Fig. 11) validated this approach (e.g. Angelier, 1994; Twiss and Unruh, 1998).

While the faults are not organized with respect to structural position, they are well organized stratigraphically. Overall, contraction faults increase in abundance up-section and are absent in the stratigraphically lowest stations in both studied areas. Extensional faults of various orientations are more dominant in fold cores, but occur with less abundance up-section (Figs. 7 and 8). This inner-arc extension and outer-arc shortening manifested by the mesoscopic faults are inconsistent with buckling and finite-neutral surface development expected during parallel folding (e.g. Hudleston and Lan, 1994).

Stratigraphically lower positions within the Guarga Formation in both regions (stations 1, 2, and 3 at Boltaña,

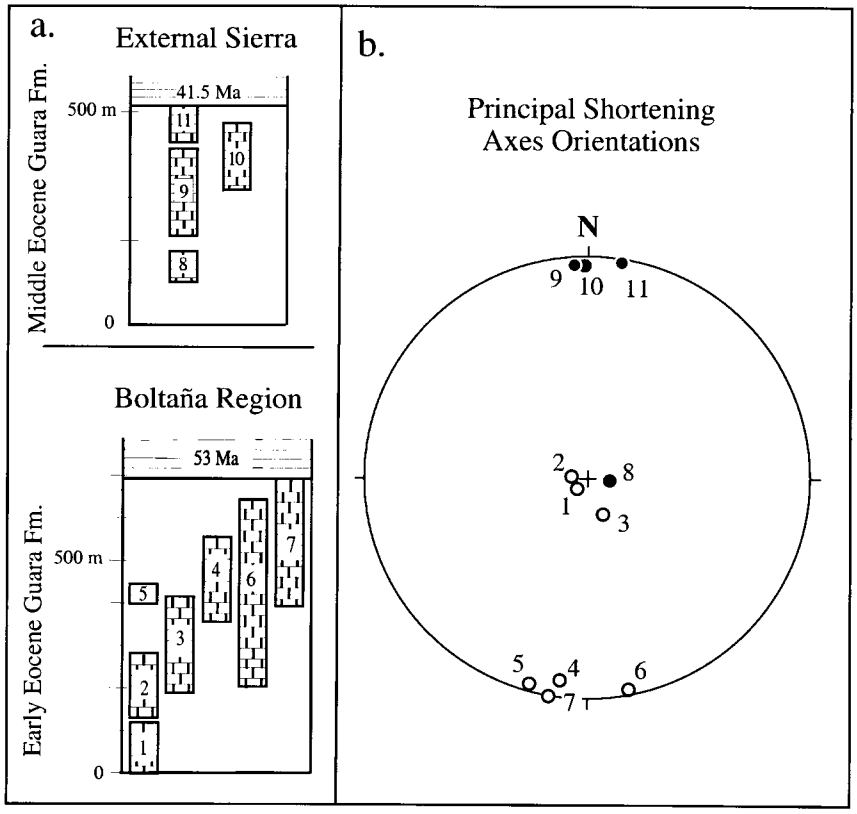

Fig. 11. Summary of principal shortening directions and their stratigraphic distribution in the Guara Formation. (a) Stratigraphic interval for each station shown within Boltaña and External Sierra measured sections of Guara Formation. Age of overlying flysch shown. Note that the relatively older stratigraphic sites (1, 2, 3, and 8) record steep shortening directions, while relatively younger stratigraphic positions (5, 6, 7, 9, 10, and 11) record NNE–SSW horizontal shortening. Solid dots: External Sierra stations; open circles: Boltaña stations.

and 8 at External Sierra) are characterized by steep shortening axes. Stratigraphically higher locations (stations 4, 5, 6, and 7 at Boltaña, and 9, 10, and 11 at External Sierra) record shortening oriented NNW–SSW horizontal (Fig. 11). We interpret the change in strain axis orientation in the syntectonic Guara Formation to provide a chronologic perspective on changing deformation regimes. Guara Formation deposition, halotectonic deformation, and thrusting were diachronous across the region, so the kinematic patterns developed at different times in the two regions (Figs 4b and 11). Halotectonic folding migrated from east to west, whereas thrusting migrated from northeast to southwest across the foreland (Anastasio, 1992). In the east, halotectonic folding preceded thrusting locally, whereas in the west, halotectonic folding occurred within the active Guarga thrust sheet (Anastasio, 1992). The steep shortening axes are consistent with diapiric folding (e.g. Schwerdtner et al., 1978), but not with lateral thrust emplacement (e.g. Séguret, 1972; Déramond and Hossack, 1984; Nichols, 1984; Hirst and Nichols, 1986). The NNE–SSW horizontal shortening axes are, however, consistent with emplacement of the Guarga thrust sheet (Figs. 5 and 6).

The shift from steep to shallow principal shortening axes is very abrupt in the Guara Formation in both regions, even though transverse folding continued during thrust sheet emplacement (Fig. 4b). The age of the Guara Formation within each area is only broadly constrained by biostratigraphy (Pocovi, 1979; Barnolas and Teixell, 1994) and the base of overlying flysch is a disconformity with an unknown age gap (Puigdefabregas, 1975), so the age of the kinematic change in each field area is not currently discernible.

6. Conclusions

Mesoscopic deformation in the southern Pyrenees occurred by faulting. Extensional faults of varied orientation predominate at lower stratigraphic levels and accommodated crestal extension over halotectonic décollement anticlines. Contractional and strike-slip faults characterize higher stratigraphic levels and are related to thrusting. Kinematic analysis of fault-slip data elucidate a shift in the orientation of maximum shortening axes from steep in older strata to NNE–SSW horizontal at younger stratigraphic levels in the syntectonic Guara Formation. The change in kinematic axis orientation up-section is interpreted to reflect a change in deformation regime from one dominated by differential loading halotectonics to one dominated by thrust tectonics during the Eocene.

Acknowledgements

Fieldwork was supported by National Science Foundation Grant EAR-8816335 awarded to DJA. Jake Hossack, Rod Graham, and Jo Déramond are thanked for introducing DJA to the Spanish Pyrenees. Careful editing by Bill Dunne and thorough reviews by Rick Allmendinger and Jonathan Turner improved the clarity of the paper and are appreciated.

References

Allmendinger, R.W., Marrett, R.R., Cladouhos, T., 1992. FaultKin, version 3.25, a program for analyzing fault slip data for the Macintosh™ computer. Cornell University, Ithaca, NY.

Almela, A., Rios, J., 1952. Estudio geologico de la zona Subpirenaica Aragonesa y de sus Sierras Marginales. Acta I Congresso Internacional Estudios Pirenaicos 1, 327–350.

Anastasio, D.J., 1987. Thrusting, halotectonics and sedimentation in the External Sierra, Southern Pyrenees, Spain. Ph.D. thesis, Johns Hopkins University.

Anastasio, D.J., 1992. Structural evolution of the external Sierra, Spanish Pyrenees. In: Mitra, S., Fisher, G.W. (Eds.), The Structural Geology of Fold and Thrust Belts. Johns Hopkins University Press, pp. 239–251.

Anastasio, D.J., Fisher, D.M., Messina, T.A., Holl, J.E., 1997. Kinematics of décollement folding in the Lost River Range, Idaho. Journal of Structural Geology 19, 355–368.

Angelier, J., 1990. Inversion of field data in fault tectonics to obtain regional stress. III. A new rapid direct inversion method by analytical means. Geophysical Journal International 103, 363–376.

Angelier, J., 1994. Fault slip analysis and paleostress reconstruction. In: Hancock, P.L. (Ed.), Continental Deformation. Pergamon Press, Oxford, pp. 53–100.

Angelier, J., Barrier, E., Chu, H.T., 1986. Plate collision and paleostress trajectories in a fold-thrust belt: the foothills of Taiwan. Tectonophysics 125, 161–178.

Angelier, J., Mechler, P., 1977. Sur une methode graphique de recherche des contraintes principales egalement utilisable en tectonique et en seismologie: la methode des diedres droits. Bulletin de la Societe Geologique de France 7, 1309–1318.

Aydin, A., Reches, Z., 1982. Number and orientations of fault sets in the field and in experiments. Geology 10, 110–112.

Barnolas, A., Teixell, A., 1994. Platform sedimentation and collapse in a carbonate-dominated margin of a foreland basin (Jaca basin, Eocene, Southern Pyrenees). Geology 22, 1107–1110.

Bielenstein, H.U., 1969. The Rundle thrust sheet, Banff, Alberta. Ph.D. thesis, Queen's University.

Boyer, S.E., 1978. Structure and origin of the Grandfather window, North Carolina. Ph.D. thesis, Johns Hopkins University.

Cámara, P., Klimowitz, J., 1985. Interpretacion geodinámica de la vertiente centro-occidental Surpirenaica (Cuenca de Jaca-Tremp). Estudios Geológicos 41, 391–404.

Choukroune, P., Séguret, M., 1973. Tectonics of the Pyrenees: role of compression and gravity. In: DeJong, K.A., Scholten, R. (Eds.), Gravity and Tectonics. John Wiley, New York, pp. 141–156.

Cloos, E., 1961. Bedding slips, wedges, and folding in layered sequences. Geological Society of Finland Bulletin 33, 105–122.

Contribucion de la Exploracion Petrolifera al Conocimiento de la Geologia de Espana, 1987. Publications of the Instituto Geologico y Minero de España.

Dahlen, F.A., Suppe, J., Davis, D.M., 1984. Mechanics of fold-and-thrust belts and accretionary wedges: cohesive Coulomb theory. Journal of Geophysical Research 89, 10087–10101.

Dahlstrom, C.D.A., 1970. Structural geology in the eastern margin of the Canadian Rocky Mountains. Canadian Society of Petroleum Geologists Bulletin 18, 332–406.

Daignieres, M., Gallart, J., Banda, E., Hirn, A., 1981. Implications of the seismic structure for the orogenic evolution of the Pyrenean Range. Earth and Planetary Science Letters 57, 88–100.

Davis, D.M., Engelder, T., 1987. Thin-skinned deformation over salt. In: Lerche, I., O'Brien, J.J. (Eds.), Dynamical Geology of Salt and Related Structures. Academic Press, Orlando, pp. 301–337.

DePaor, D.G., Anastasio, D.J., 1987. The external Sierra: a case history in the advance and retreat of mountains. National Geographic Research 3, 199–209.

Déramond, J., Hossack, J.R., 1984. In: Déramond, J., Fischer, M., Hossack, J., Labaume, P., Seguret, M., Soula, J.-C., Villard, P., Williams, G. (Eds.), Field Guide of Conference Trip to the Pyrenees. Chevauchement et Deformation Conference, Toulouse.

Déramond, J., Graham, R.H., Hossack, J.R., Baby, P., Crouzet, G., 1985. Nouveau modele de la chaine des Pyrenees. Comptes Rendus de l'Academie des Sciences, Paris 301, 1212–1216.

Diegel, F.A., 1988. The Rome Formation décollement in the Mountain City window, Tennessee; a case for involvement of evaporites in the genesis of Max Meadows-type breccias. In: Mitra, G., Wojtal, S. (Eds.), Geometries and Mechanisms of Thrusting with Special Reference to the Appalachians. Geological Society of America Special Paper 222, pp. 137–164.

Durney, D.W., Ramsay, J.G., 1973. Incremental strains measured by syntectonic crystal growths. In: De Jong, K.A., Scholten, R. (Eds.), Gravity and Tectonics. John Wiley, New York, pp. 67–96.

ECORS Pyrenees Team, 1988. Deep reflection seismic survey across an entire orogenic belt, the ECORS Pyrenees profile. Nature 331, 508–511.

Etchcopar, A., Vasseur, G., Daignieres, M., 1981. An inverse problem in microtectonics for the determination of stress tensors from fault striation analysis. Journal of Structural Geology 3, 51–65.

Gapais, D., Cobbold, P.R., Bourgeois, O., Rouby, D., de Urreiztieta, M., 2000. Tectonic significance of fault-slip data. Journal of Structural Geology 22, 881–888.

Garrido-Megias, A., Camara, R.P., 1983. Direction and displacement of tectonic units in the southern Pyrenees, the tectonic evolution of the Pyrenees: a workshop, Cambridge University conference report. Journal of the Geological Society, London 141, 379–381.

Grimaud, S., Boillot, G., Collette, B.J., Mauffret, A., Miles, P.R., Roberts, D.G., 1982. Western extension of the Iberian–European plate boundary during the early Cenzoic (Pyrenean) convergence: a new model. Marine Geology 45, 63–77.

Hancock, P.L., 1985. Brittle microtectonics: principles and practice. Journal of Structural Geology 7, 437–457.

Hirst, J.P.P., Nichols, G.J., 1986. Thrust tectonic controls on Miocene alluvial distribution patterns, southern Pyrenees. In: Allen, P.A., Homewood, P. (Eds.), Foreland Basins. International Association of Sedimentologists Special Publication 8. Blackwell Scientific, Oxford, pp. 247–258.

Hoeppener, R., 1955. Tektonik im Schiefergebirge. Geologische Rundshau 44, 26–58.

Hogan, P.J., Burbank, D.W., 1996. Evolution of the Jaca piggyback basin and emergence of the external Sierra, southern Pyrenees. In: Friend, P.F., Dabrio, C.J. (Eds.), Tertiary Basins of Spain: the Stratigraphic Record of Crustal Kinematics. Cambridge University Press, Cambridge, pp. 153–160.

Holl, J.E., Anastasio, D.J., 1992. Deformation of a foreland carbonate thrust system, Sawtooth Range, Montana. Geological Society of America Bulletin 104, 944–953.

Holl, J.E., Anastasio, D.J., 1995aa. Kinematics around a large-scale oblique ramp, southern Pyrenees, Spain. Tectonics 14, 1368–1379.

Holl, J.E., Anastasio, D.J., 1995bb. Cleavage development within a foreland fold and thrust belt, Southern Pyrenees, Spain. Journal of Structural Geology 17, 357–369.

Hudleston, P.J., Lan, L., 1994. Rheological controls on the shapes of single-layer folds. Journal of Structural Geology 16, 1007–1021.

Jackson, M.P.A., Talbot, C.J., 1994. Advances in salt tectonics. In: Hancock, P.L. (Ed.), Continental Deformation. Pergamon Press, Oxford, pp. 159–179.

Jenyon, M.K., 1986. Salt Tectonics. Elsevier, London.

Kleinspehn, K.L., Pershing, J., Teyssier, C., 1989. Paleostress stratigraphy: a new technique for analyzing tectonic control on sedimentary-basin subsidence. Geology 17, 253–256.

Krantz, R.W., 1988. Multiple fault sets and three-dimensional strain: theory and application. Journal of Structural Geology 10, 225–237.

Labaume, P., Seguret, M., Seyve, C., 1985. Evolution of a turbiditic foreland basin and analogy with an accretionary prism: example of the Eocene south-Pyrenean basin. Tectonics 4, 661–685.

Lisle, R.J., 1987. Principal stress orientations from faults: an additional constraint. Annales Tectonicae 1, 155–158.

MacKenzie, D.P., 1969. The relationship between fault plane solutions for earthquake and the directions of the principal stresses. Bulletin of the Seismological Society of America 59, 591–601.

Marrett, R., Allmendinger, R.W., 1990. Kinematic analysis of fault-slip data. Journal of Structural Geology 12, 973–986.

Martinez, B., 1991. La Estructura Del Limite Occidental De La Unidad Surpirenaica Central. Ph.D. thesis, Universidad De Zaragoza.

Meigs, A.J., 1997. Sequential development of selected Pyrenean thrust faults. Journal of Structural Geology 19, 481–502.

Mey, P.H.W., Nagtegaal, P.J.C., Robert, K.J., Hartevelt, J.A.A., 1968. Lithostratigraphic subdivision of post-Hercynian deposits in the south central Pyrenees, Spain. Leidsche Geologische Mededelingen. 41, 221–228.

Müller, W.H., 1982. Zur Entstehung der Rauhwacken. Ecologae Geologica Helvetiae 75, 481–494.

Muñoz, J., 1992. Evolution of a continental collision belt: ECORS-Pyrenees crustal balanced cross section. In: McClay, K.R. (Ed.), Thrust Tectonics. Chapman & Hall, New York, pp. 235–246.

Nichols, G.J. 1984. Thrust tectonics and alluvial sedimentation, Aragon, Spain. Ph.D. thesis, Cambridge University.

Nickelsen, R.P., Hough, V.N.D., 1967. Jointing in the Appalachian Plateau of Pennsylvania. Geological Society of America Bulletin 78, 609–630.

Norris, D.K., 1958. Structural conditions in Canadian coal mines. Geologic Survey of Canada Bulletin 44.

Pocovi, A.J., 1979. Estudio geologico de las Sierras Marginales Catalanas (Prepirineo de Lerida). Acta Geologica Hispanica 13, 73–79.

Price, R.A., 1967. The tectonic significance of mesoscopic subfabrics in the Southern Rocky Mountains of Alberta and British Columbia. Canadian Journal of Earth Sciences 4, 39–70.

Pueyo, E.L., Millan, H., Pocovi, A., 2000. Rotation velocity of a thrust: a magnetotectonic study in the Pico del Aguila anticline (Southern Pyrenees Spain). Sedimentary Geology, Special Issue on Growth Strata.

Puigdefabregas, C.T., 1975. La sedimentation Molasica en la cuenca de Jaca. Monografias del instituto de estudion Pirenaicos 104.

Reches, Z., 1978. Analysis of faulting in a three-dimensional strain field. Tectonophysics 47, 109–129.

Rocher, M., Lacombe, O., Angelier, J., Deffontaines, X., Verdier, F., 2000. Cenozoic folding and faulting in the south Aquitaine basin (France): insights from combined structural and paleostress analysis. Journal of Structural Geology 22, 627–645.

Roest, W.R., Srivastava, S.P., 1991. Kinematics of the plate boundaries between Eurasia, Iberia, and Africa in the North Atlantic from Late Cretaceous to the present. Geology 19, 613–616.

Roure, F., Choukroune, P., Berastegui, X., Muñoz, J.A., Villien, A., Matheron, P., Bareyt, M., Séguret, M, Cámara, P., Déramond, J., 1989. ECORS deep seismic data and balanced cross sections: geometric constraints on the evolution of the Pyrenees. Tectonics 8, 41–50.

Schwerdtner, W.M., Sutcliffe, R.H., Troeng, B., 1978. Patterns of total strain in the crestal region of immature diapirs. Canadian Journal of Earth Sciences 15, 1437–1447.

Séguret, M., 1972. Etude tectonique des nappes et series decollees de la partie centrale du versant sud des Pyrenees, caractere synsedimentaire role de la compression et de la gravite. Publications de L'universite des sciences et techniques du languedoc (USTELA), Montpellier-Serie Geol. Struct., no. 2.

Stearns, D.W., 1969. Fracture as a mechanism of flow in naturally deformed layered rocks. Research in Tectonics, Geological Survey of Canada Paper 68-52, pp. 79–95.

Teixell, A., 1996. The Anso transect of the southern Pyrenees: basement and cover thrust geometries. Journal of the Geological Society, London 153, 301–310.

Thomas, J.C., Gapais, D., Cobbold, P.R., Meyer, V., Burtman, V.S., 1996. Tertiary kinematics of the Tadjik depression (central Asia): inferences from fault and fold patterns. In: Roure, F., Ellouz, N., Shein, V.S., Skvorstov, I.I. (Eds.), Geodynamic Evolution of Sedimentary Basins. Editions Technip, Paris, pp. 171–180.

Turner, J.P., Hancock, P.L., 1990. Relationship between thrusting and joint systems in the Jaca thrust-tip basin, Spanish Pyrenees. Journal of Structural Geology 12, 217–226.

Twiss, R.J., Unruh, J.R., 1998. Analysis of fault slip inversions: do they constrain stress or strain rate? Journal of Geophysical Research 103, 12205–12222.

Will, T.M., Powell, R., 1991. A robust approach to the calculation of paleostress fields from fault plane data. Journal of Structural Geology 13, 813–821.

Wojtal, S., 1986. Deformation within foreland thrust sheets by populations of minor faults. Journal of Structural Geology 8, 341–360.

Zwart, H.J., 1979. The geology of the central Pyrenees. Leidse Geologische Mededelingen 50, 1–74.